Anticorrosive Effect and Catalytic Activity of a Newly Synthesized Chalcone and its Copper Complex: Application Studies

Ahmed M. El-desoky[b], Dina M. Abd El-Aziz[a], Marwa N. El-Nahass*[a]

[a]Chemistry Department, Faculty of Science, Tanta University, 31527 Tanta, Egypt
[b]Engineering Chemistry Department, High Institute of Engineering &Technology (New Damietta), Egypt and
Al-Qunfudah Center for Scientific Research (QCSR), Al-Qunfudah University College, Umm Al-Qura University, KSA

Abstract—The inhibitory action of newly synthesized chalcone against the corrosion of copper in 1 M HNO_3 solution was investigated using Tafel polarization and electrochemical impedance spectroscopy (EIS) techniques. The inhibition efficiency increased with increasing inhibitor concentrations. Molecular modelling was used to gain some insight, about structural and electronic effects in relation to the inhibiting efficiencies. On the other hand, advanced oxidation processes (AOPs) have proved very effective in the treatment of the various hazardous organic pollutants in water. The synthesized complex was found to be quite active for the catalytic degradation of the Acid Blue 25 textile dye and could be a potential model for removal dyes from colored effluents. Catalytic degradation of the Acid Blue 25 textile dye was studied using H_2O_2 as oxidant and copper-chalcone complex as heterogenous catalyst using steady-state absorption and emission techniques. The mechanism of the degradation process involves an electron excitation and the generation of very active oxygenated species that attack the dye molecules. The percent of degradation obtained after the reaction between the acid blue 25 dye and both H_2O_2/catalyst was 86.7, while the corresponding one with catalyst only was 74.6. Finally, the reusability of the catalyst, copper-chalcone complex has been reported.

Index Terms— EIS, Cu(II)- Chalcone complex, Catalytic degradation, Anticorrosive effect, Acid blue 25

—————————— ◆ ——————————

1 INTRODUCTION

Copper is widely used in many applications in microelectronic industries and communication as a conductor in electrical power lines, pipelines for domestic and industrial water utilities including sea water, heat conductors and fabrication of heat exchangers due to its excellent electrical and thermal conductivities, low cost and its good mechanical workability [1,2]. Therefore, considerable attention has been drawn during the past few decades to inhibit corrosion of copper. Corrosion inhibition of copper can be achieved through the modification of its interface by forming self assembled ordered ultra thin layers of organic inhibitors. It is well known that Copper exists as a divalent ion in water. Copper rarely occurs naturally in drinking water. Levels over 0.05 mg/L are not naturally encountered in drinking water. The presence of excess copper can occur as a result of corrosion in the water system or can be from industrial discharges or from copper salts used for algae control in reservoirs. Too much copper in the human body can cause stomach and intestinal distress such as nausea, vomiting, diarrhea, and stomach cramps. To overcome of this problem, organic compounds have been used as corrosion inhibitors for copper and copper based alloys. Among the wide chemical organic compounds are chalcones which have recently been investigated as corrosion inhibitors for various metals and alloys in acid media [3,4]. These substances generally become effective by adsorption on the metal surface. The

adsorbed species protect the metal from the aggressive medium, which causes decomposition of the metal, but also on the chemical structure of the inhibitor [5-8].

Also, the presence of a large quantity of organic wastewaters generated by carpet, dyeing, textile, pulp, and paper industries became a big environmental problem [9]. It was estimated that approximately 1-15% of the dye is lost during dyeing and finishing processes and released, generating large amounts of wastewaters [10]. As a consequence, it is a great need to treat dye effluents discharging the effluent to the environment to avoid health hazards and destruction of the ecosystem. Various physic-chemical and biological methods have been used in order to remove dyes from colored effluents [11]. These methods are efficient; however, the major constraints are the secondary pollution problem such as sludge and polluting agent transformation from one phase to another phase. Therefore, attention has to be focused on techniques that lead to the complete degradation of pollutants [12]. The AOP techniques are widely used for the removal of recalcitrant organic constituents from industrial and municipal wastewater [13]. In this sense, AOPs type procedures can become very promising technologies for treating wastewater containing non-biodegradable or hardly biodegradable organic compounds with high toxicity. These procedures are based on generating highly oxidative hydroxyl radicals in the reaction medium.

AOP reactions make use of transition metal ions (mostly

Copper) in combination with ligand molecules for the decomposition of hydrogen peroxide and the resulting production of hydroxyl radicals. Copper(II) complex systems have been used for the degradation of lignin [14], polycyclic aromatic hydrocarbons [15], and synthetic dyes [16,17]. Hence, researchers are keen to search for a low-molecular weight ligand with high decolonization efficiency to be used in these reactions and to demonstrate the involvement of hydroxyl radicals in the decolonization reaction.

Synthetic dyes are preferred for use over natural dyes due to their superior performance. As compared to natural dyes, synthetic dyes impart brighter colors, show better light-fastness and are more resistant to washing. Wastewater or effluents from industries that manufacture paints, pigments and color cosmetics contain a variety of synthetic dyes. Anthraquinonic dyes feature among the most widely used synthetic dyes in industry globally after azo-compounds and are mainly used for dyeing wool, polyamide and leather [18]. One of the noticeable anthraquinoic dye is Acid Blue 25, which was chosen because of its known wide applications (wool, nylon, silk, paper, ink, aluminum, detergent, wood, fur, cosmetics and biological stain) and causes skin, eye irritation and may also create respiratory problem [19]. Thus the decontamination of this dye is major concern to the environmentalists.

Herein, the inhibiting action of a newly synthesized chalcone on the corrosion of copper was reported. The electrochemical techniques such as polarization measurements and electrochemical impedance spectroscopy (EIS) were used in this study. Differences in behavior of inhibitor were explained based on the structural properties of the investigated inhibitor and by using quantum calculations. On the other hand, the kinetics of catalytic degradation of acid blue 25 dye with H_2O_2 catalyzed by the synthesized copper-chalcone complex was investigated.

2. Experimental

2.1. Materials

All chemicals were obtained from Merck-Aldrich Chemical and used without purification. They include 2-acetyl pyridine, 4-(dimethyl amino)-cinnamaldehyde, a metal chloride ($CuCl_2 \cdot 2H_2O$). Hydrogen peroxide (30% w/v, Merck) was used. The initial concentration of H_2O_2 was determined iodometrically using the standard $Na_2S_2O_3$ solution in the presence of starch as an indicator. The desired concentration of H_2O_2 was obtained by successive dilution from the standard stock solution. Acid blue 25 [1-amino-9,10-dihydro-9,10-dioxo-4-(phenylamino)-2-anthracenesulfonic acid, monosodium salt] (molecular formula: $C_{20}H_{13}N_2NaO_5S$) was supplied from Aldrich and is used without further purification. The structural formula of this dye is shown in Scheme 1. The solvent, ethanol (EtOH, HPLC) was used as received. Deionized water was used to make the dye solutions of the desired concentration.
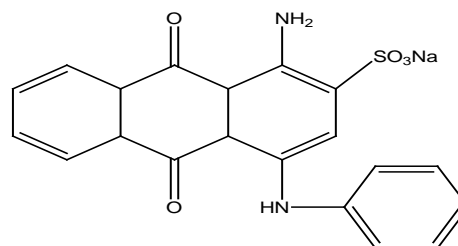

Scheme 1. Structure of acid blue 25. Preparation of the corrosion inhibitor, chalcone and the catalyst, copper-chalcone complex

The corrosion inhibitor, chalcone as well as the catalyst, copper-chalcone complex, were synthesized according to the method reported previously [20]. The obtained chalcone and its complex were characterized using FT-IR analysis, Mass spectra, thermogravimetric analysis (TGA). The structure of the investigated chalcone and its complexes were shown in Schemes 2 and 3.
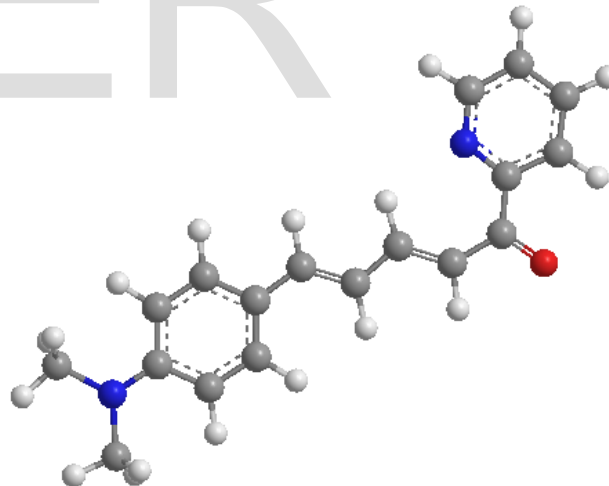
Scheme 2. The structure of the corrosion inhibitor, chalcone.
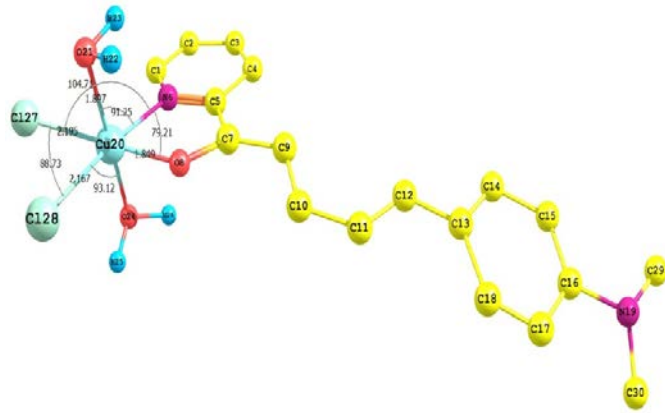
Scheme 3. 3D structure of the investigated catalyst, copper-chalcone complex.

2.2. Corrosion Measurements

2.3.1. Materials

Tests were performed on copper of the following composition (weight %): 0.027 % Ni, 0.067 % Zn, 0.006 % Se, and the remainder Cu (99.90 %).

2.3.2. Solutions

The aggressive solutions, 1 M HNO_3 were prepared by dilution of BDH grade (70 %) HNO_3 with demineralized water. The concentration range of the inhibitors used was 1×10^{-7} - 5×10^{-5} M.

2.3.3. Potentiodynamic Polarization Measurements

Polarization experiments were carried out in a conventional three-electrode cell with a platinum counter electrode and a saturated calomel electrode (SCE) coupled to a fine Luggin capillary as the reference electrode. The working electrode was in the form of a square cut from copper embedded in epoxy resin of polytetrafluoroethylene (PTFE) so that the flat surface was the only surface in the electrode. The working surface area was 1.0×1.0 cm². Tafel polarization curves were obtained by changing the electrode potential automatically from -600 to +400 mV at open circuit potential with a scan rate of 1 mVs⁻¹. Stern-Geary method [21] used for the determination of corrosion current is performed by extrapolation of anodic and cathodic Tafel lines to a point which gives log i_{corr} and the corresponding corrosion potential (E_{corr}) for inhibitor free acid and for each concentration of inhibitor. Then i_{corr} was used for calculation of inhibition efficiency and surface coverage (θ) as below:

IE % = θ x 100 = [1- ($i_{corr(inh)}$ / $i_{corr(free)}$)] × 100

(1)

Where $i_{corr(free)}$ and $i_{corr(inh)}$) are the corrosion current densities in the absence and presence of inhibitor, respectively.

2.3.4. Electrochemical Impedance Spectroscopy Measurements

Impedance measurements were carried out in frequency range from 100 kHz to 10 mHz with amplitude of 5 mV peak-to-peak using ac signals at open circuit potential. The experimental impedance were analyzed and interpreted on the basis of the equivalent circuit. The main parameters deduced from the analysis of Nyquist diagram are the resistance of charge transfer R_{ct} (diameter of high frequency loop) and the capacity of double layer C_{dl} which is defined as:

$$C_{dl} = 1/ (2 \pi f_{max} R_{ct}) \tag{2}$$

The inhibition efficiencies and the surface coverage (θ) obtained from the impedance measurements are defined by the following relation [22]:

$$\%IE = \theta \times 100 = [1- (R°_{ct}/R_{ct})] \times 100 \tag{3}$$

Where R_{oct} and R_{ct} are the charge transfer resistance in the absence and presence of inhibitor, respectively.

2.3.5. Theoretical Study

Accelrys (Material Studio Version 4.4) software for quantum chemical calculations has been used.

2.4 Kinetic Measurements

In typical kinetic run, a number of conical flasks (100 ml) containing a definite quantity of the solid catalyst together with the appropriate volume of distilled H_2O were placed in a water shaker thermostat in order to attain the desired temperature. To each conical flask, an appropriate volume of the separated thermostated dye and H_2O_2 solutions were added and zero time was noted. At regular time intervals aliquots of each conical flask were withdrawn and the absorbance was recorded at the corresponding λ_{max} = 615 nm of the dye. Generally, the dye/ H_2O_2 mixture was stable for several hours without any noticeable change in the absorbance of dye, which indicates that no reaction takes place between the dye and H2O2 in the absence of the complex.

The kinetic measurements were carried out spectrophotometrically using a Shimadzu UV-3101PC scanning spectrophotometer. It is equipped with an electronically temperature control unit (TCC-260) to maintain constant temperature with an accuracy ± 0.1°C. Fluorescence spectra were measured using a Perkin–Elmer LS 50B spectrofluorometer. A shaker water thermostat (Julabo SW20 C) was used to shake the heterogeneous reaction mixture at 120 rpm at fixed temperature ± 0.1 ∘C.

3. Results and Discussion

3.1. Potentiodynamic Polarization Measurements

Fig.1 shows the anodic and cathodic Tafel polarization curves for copper in 1 M HNO_3 in the absence and presence of varying concentrations of the inhibitor at 25∘C. It is clearly that both anodic metal dissolution and cathodic reduction reactions were inhibited when inhibitor was added to 1 M HNO_3 and this inhibition was more pronounced with increasing inhibitor concentration. Tafel lines are shifted to more negative and more positive potentials with respect to the blank curve by increasing the concentration of the inhibitor. This behavior indicates that the undertaken additive act as mixed-type inhibitor [23, 24]. The results show that the increase in inhibitor concentration leads to decrease the corrosion current density (i_{corr}) as shown from Table 1, but the Tafel slopes (βa , βc), are approximately constant indicating

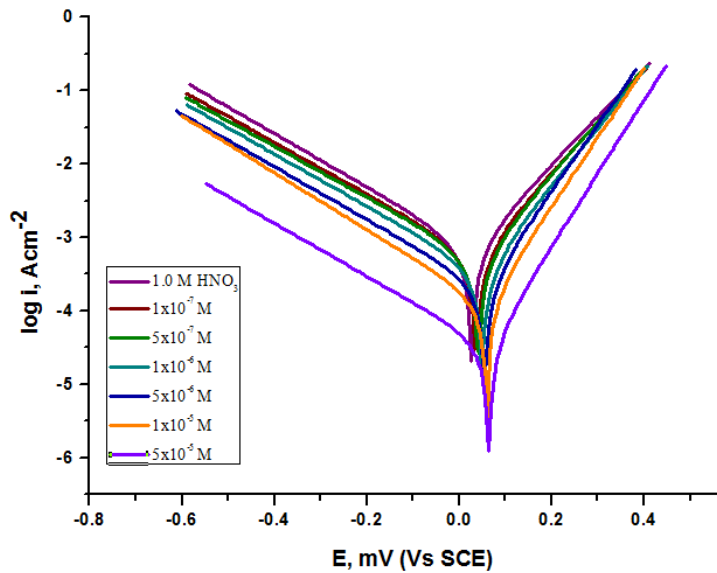that the retardation of the two reactions were affected without changing the dissolution mechanism [25-27].

Fig.1 Potentiodynamic polarization curves for corrosion of copper in 1 M HNO_3 in the absence and presence of different concentrations of inhibitor at 25°C.

TABLE 1. POTENTIODYNAMIC POLARIZATION PARAMETERS FOR COPPER IN 1 M HNO_3 CONTAINING VARIOUS CONCENTRATIONS OF INHIBITOR AT 25 °C.

Conc., M	$E_{corr.}$ mV (vs SCE)	i_{corr} $\mu A\ cm^{-2}$	β_c mV dec^{-1}	β_a mV dec^{-1}	θ	IE %
0.0	28.4	741.3	269	161	-	-
1×10^{-7}	34.9	583.2	287	155	0.213	21.3
5×10^{-7}	42.4	519.8	282	141	0.298	29.8
1×10^{-6}	51.4	351.7	279	132	0.525	52.5
5×10^{-6}	56.4	222.1	283	121	0.700	70.0
1×10^{-5}	59.2	129.5	261	113	0.825	82.5
5×10^{-5}	65.0	53.7	271	114	0.927	92.7

3.2. Electrochemical Impedance Spectroscopy (EIS)

The effect of inhibitor concentration on the impedance behavior of copper in 1 M HNO_3 solution at 25°C is presented in Fig.2. The curves show a similar type of Nyquist plots for copper in the presence of various concentrations of inhibitor. The existence of single semi-circle show the single charge transfer process during dissolution. This is unaffected by the presence of inhibitor molecules. Deviations from perfect circular shape are often referred to the frequency dispersion of interfacial impedance which arises due to surface roughness, impurities, dislocations, grain boundaries, adsorption of inhibitors, and formation of po-

rous layers and in homogenates of the electrode surface [28, 29]. The electrical equivalent circuit model is shown in Figure 3. It is used to analyze the obtained impedance data. The model consists of the solution resistance (R_s), the charge-transfer resistance of the interfacial corrosion reaction (R_{ct}) and the double layer capacitance (C_{dl}). Excellent fit with this model was obtained with our experimental data. EIS data (Table 2) show that the R_{ct} values increases and the C_{dl} values decreases with increasing the inhibitor concentrations. This is due to the gradual replacement of water molecules by the adsorption of the inhibitor molecules on the metal surface, decreasing the extent of dissolution reaction. The high (R_{ct}) values, are generally associated with slower corroding system [30, 31]. The decrease in the C_{dl} can result from the decrease of the local dielectric constant and/or from the increase of thickness of the electrical double layer suggested that the inhibitor molecules function by adsorption at the metal/solution interface [32]. The % IE obtained from EIS measurements are close to those deduced from polarization measurements.
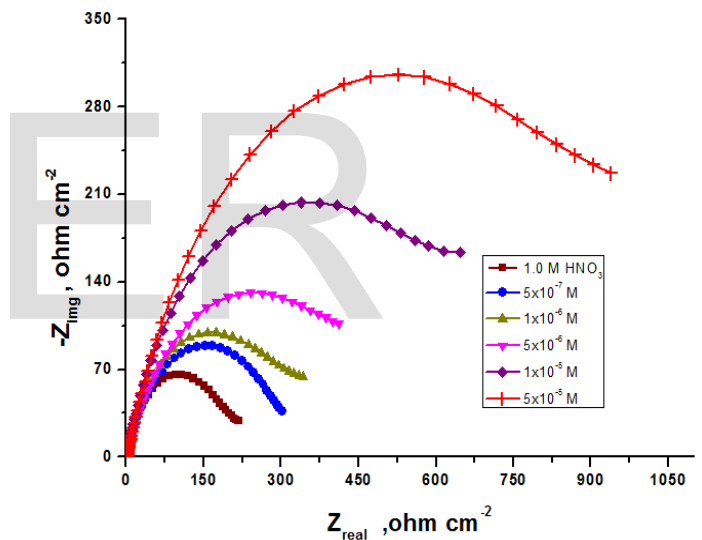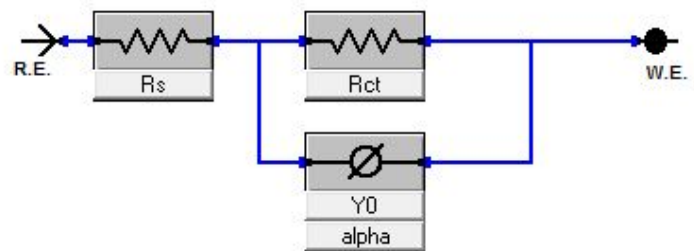

Fig 2 Nyquist plot for copper in 1 M HNO_3 in the absence and presence of different concentrations of the inhibitor at 25 °C.

Fig 3 Electrical equivalent circuit model used to fit the results of impedance.

TABLE 2. EIS DATA OF COPPER IN 1 M HNO$_3$ AND IN THE ABSENCE AND PRESENCE OF DIFFERENT CONCENTRATIONS OF OF THE INHIBITOR AT 25 °C.

Conc., M	R_S, Ω cm^2	Y_0, $\mu\Omega^{-1}$ s^n cm^{-2}	n	R_{ct}, Ω cm^2	C_{dl}, μF cm^{-2}	θ	IE %
0.0	1.599	503.4	0.781	205.6	98.1	-	-
1×10^{-7}	1.212	320.7	0.792	334.6	42.9	0.386	38.6
5×10^{-7}	1.261	262.4	0.752	391.2	30.31	0.474	47.4
1×10^{-6}	1.378	160.2	0.726	662.1	18.7	0.689	68.9
5×10^{-6}	1.549	122.8	0.714	891.4	13.8	0.769	76.9
1×10^{-5}	1.617	72.4	0.797	1551	11.1	0.867	86.7
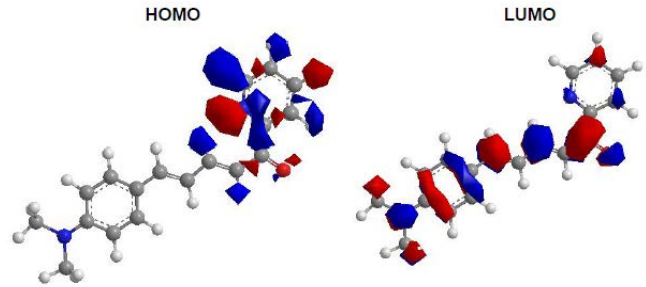
Fig 4 Molecular orbital plots and Mulliken charges of the synthesized chalcone.

3.3. Quantum Chemical Calculations

Theoretical calculations were performed for only the neutral forms, in order to give further insight into the experimental results. Fig. 4 represents the molecular orbital plots of the investigated compound. Values of quantum chemical indices such as energies of lowest unoccupied molecular orbitals (LUMO) and energy of highest occupied molecular orbitals (HOMO), E_{HOMO} and E_{LUMO}, the formation heat ΔH_f and energy gap ΔE, are calculated by semi-empirical AM1, MNDO and PM3 methods has been given in Table 3. It has been reported that the higher or less negative E_{HOMO} is associated of inhibitor, the greater the trend of offering electrons to unoccupied d orbital of the metal, and the higher the corrosion inhibition efficiency, in addition, the lower E_{LUMO}, the easier the acceptance of electrons from metal surface [33]. From Table 3, it is clearly that ΔE obtained by the four methods in case of the inhibitor is lower, which enhance the assumption that the inhibitor molecule will absorb more strongly on copper surface, due to facilitating of electron transfer between molecular orbital HOMO and LUMO which takes place during its adsorption on the metal surface and there after presents the maximum of inhibition efficiency. Reportedly, excellent corrosion inhibitors are usually those organic compounds who are not only offer electrons to unoccupied orbital of the metal, but also accept free electrons from the metal [34, 35]. It can be seen that all calculated quantum chemical parameters validate these experimental results.

TABLE 3. THE CALCULATED QUANTUM CHEMICAL PROPERTIES FOR THE INVESTIGATED CHALCONE.

E_{HOMO} (eV)	E_{LUMO} (eV)	ΔE (eV)	X (eV)	η (eV)	σ (eV)$^{-1}$	Pi (eV)	S (eV)$^{-1}$	ω (eV)	ΔN_{max}
-7.411	-6.106	1.305	6.7585	0.6525	1.53256705	-6.7585	0.76628352	35.0017795	10.3578544

3.4. Catalytic Activity of the Catalyst, Copper-Chalcone Complex

Transition metal complexes supported on different surfaces were used as potentially active catalysts for the decomposition of H$_2$O$_2$, the oxidative degradation of organic contaminants and dyes [36]. Hence, the catalytic degradation of the Acid Blue 25 textile dye was studied using H$_2$O$_2$ as oxidant and copper-chalcone complex as heterogenous catalyst using steady-state absorption and emission techniques. When 4 mL of acid blue 25 (from 1×10^{-3} M) was mixed with 2 mL hydrogen peroxide (2 M) in a beaker containing 14 mL distilled water to get total volume of 20mL, no reaction was observed. However, when only 0.01 g of the copper-chalcone complex was added to the Acid blue 25 aqueous solution, the absorption band of acid blue 25 (at λ_{max}=615 nm) decreases gradually at various time intervals, Fig.5 (a). After 2 hrs, this band is totally disappears, confirming the complete degradation of the dye into its mineral components. On the

other hand, in the presence of both the catalyst and H_2O_2, the rapid disappears of the absorption band, Fig.5 (b). After only 50 min, the color disappears completely. This demonstrates that without the addition of copper complex, the acid blue 25 degrades in the presence of H_2O_2 but with less efficiency. Fig. 6 (a,b), shows the decreasing of absorbance at various time intervals. Also, Fig. 7, shows the decolorization of the acid blue 25 dye in the presence of the complex as a heterogenous catalyst and H_2O_2 after 10 min and 50 min.
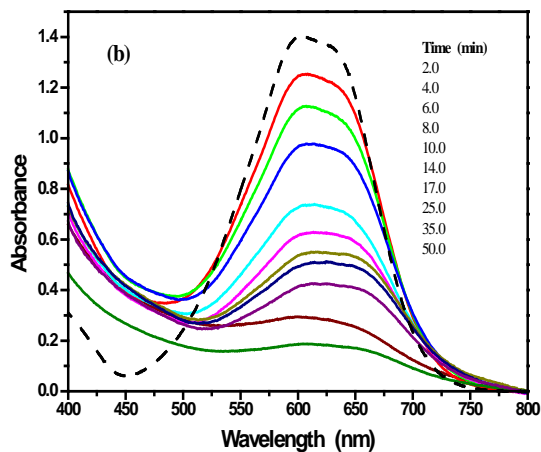

Fig.5. Time resolved absorption spectra during reaction of 2×10^{-4} M of acid blue 25 dye in the presence of (a) 0·01 g of the complex as heterogenous catalyst (a) and (b) 0·01 g of the complex as heterogenous catalyst with 0.2 M of H_2O_2.
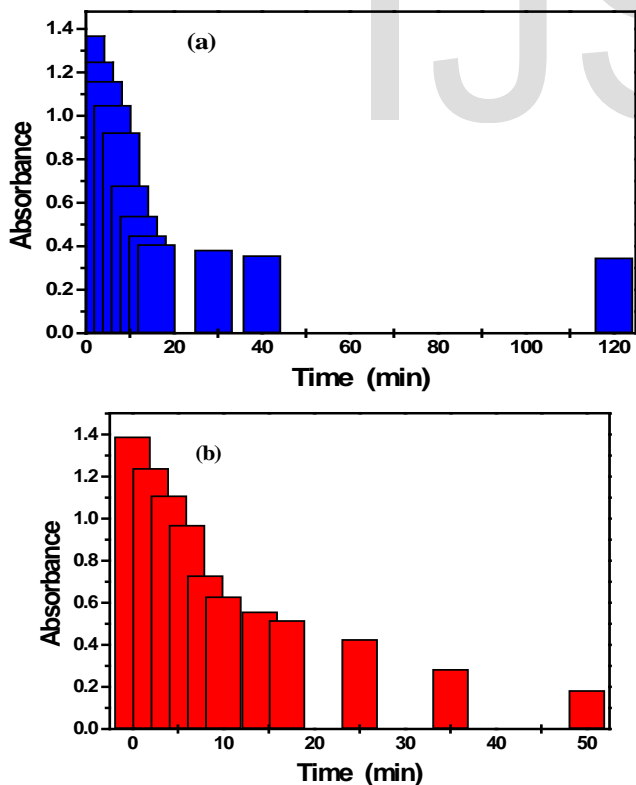

Fig. 6. The relation between the absorbance and the specific time intervals for the degradation of acid blue 25 dye in the presence of (a) the complex as heterogenous catalyst (a) and (b) the complex with H_2O_2.

Fig.7. Decolarization of (A) acid blue 25 dye in the presence of the complex as a heterogenous catalyst and H_2O_2 after 10 min (B) and 50 min (C).

The catalytic degradation percent was calculated according to the following equation [37].

$$PDP\% = \frac{A_o - A}{A_o} \times 100\% \qquad (4)$$

Where A_o is the absorbance at t=0 min and A is the absorbance at t = time, min. It was found that the percent of degradation obtained after the photocatalytic reaction between the acid blue 25 dye and both H_2O_2+catalyst was 86.7, while the corresponding one with catalyst only was 74.6. It is well known previously that H2O2 has been used for the oxidative degradation of organic dye. However, the more stable acid blue 25 dye is much more resistant to H_2O_2 oxidizer; which was confirmed by our experimental results; where there is no observed reaction. The combination of H_2O_2 and metal catalysts with the ability to form reduction and oxidation pairs has been used to degrade the organic compounds [38]. The catalytic decomposition of H_2O_2 generates free radical species like HO•, HOO•, or $O_2•$ −, and these species, especially the HO•, are the leading oxidation agent; that is to say, they are more dominant than H2O2. These species are responsible for the efficient degradation of organic dyes [39]. The copper complex may play the critical role of decomposing H2O2, and producing the free radical species as HO•, HOO•, or $O_2•$ −, that are responsible for degrading the dye molecules. However, the formation of free radical pairs is the key factor in the remarkable catalytic degradation of acid blue 25 by the used catalyst.

The main process in the degradation of acid blue 25 is the adsorption–oxidation–desorption mechanism [40]. The dye molecule and H_2O_2 were first adsorbed on the surface of the complex, and then free radical species of HO•, HOO•, or $O_2•−$ were produced by the catalytic decomposition of H_2O_2. These free radicals cause the destructive oxidation of the organic dye. The catalyst recovers immediately after desorption of the degraded dye molecules that have left the complex surface.

For the catalytic process, the best type of kinetic reaction adapted is the pseudo-first order reaction. The equation used to determine the reaction rate is based on the definition of the model. The first kinetic model is defined as [41]:

$$\ln (C_0/C) = kt \qquad (5)$$

Where C_o and C are the initial concentration and the concentration at any time, respectively. The semilogarithmic plots

of the concentrations vs time give straight lines with a good linear correlation (R₂), Fig.8. This suggests that the degradation reaction follows the first-order kinetics with respect to the acid blue 25 dye. The obtained slope represents the value of k (rate reaction). The rate constants for the dye degradation in the presence of catalyst only and catalyst+H_2O_2 were determined from the obtained slopes.
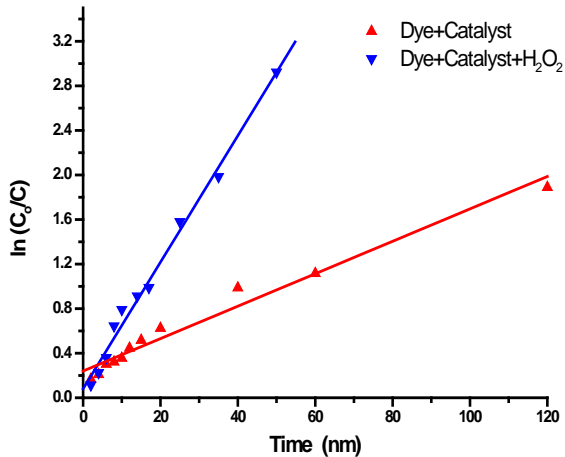

Fig 8 First-order kinetic plot of ln C_o/C_t vs. time (in min) for photocatalytic degradation of Acid blue 25 dye in the presence of the complex only as a heterogenous catalyst and in the presence of both the complex and H_2O_2 at different time intervals.

As reported, the rate constant for the degradation of the investigated dye in the presence of both H_2O_2 and the catalyst equals 0.057 min⁻¹. However, the observed rate constant for dye degradation in the presence of the catalyst only equals 0.014 min-1, indicating efficient catalysis of the complex in absence of H_2O_2 in spite of the fact that the rate of degradation is slower. Also, the observed catalytic activity could be explained on the basis of the delocalization of electrons in the conjugated metal complex as the catalytic effect which depends on the enhancement in electron-hole (e−/h+) separation [42]. On the other hand, metal complex system produced hydroxyl radicals during the catalytic reaction. This is not surprising, since the production of OH was already confirmed in other metal-based AOP systems [43]. The radicals are strong oxidizing agents that react with dye and cause its decolorization.

As known, the fluorescence spectroscopy is an important technique that has been used to determine the degradation process of the organic compounds under different catalytic processes. This technique is complementary to the UV-vis absorption technique. A decrease in the fluorescence intensity of the acid blue 25 dyes upon in the presence of catalyst and catalyst+H_2O_2 at various time intervals. Fig.9 shows the fluorescence spectra of acid blue 25 via the degradation process. In the presence of catalyst+H_2O_2, the fluorescence intensity decreased sharply to 190 (by 2.4 folds) after 10 min and then became slower after the next times within ranges 12-60 min until reach to 76 (about 5.9 folds). Additionally, an

observable bathochromic shift in the emission spectra has been found by 11 nm (located at 434nm), compared to the aqueous dye solution (located at 445nm). However, in case of using catalyst only, the fluorescence intensity decrease by 1.8 folds through the first 10 min, and after this mentioned time, the spectra decreases slowly by 5.2 folds within ranges 12-120 min. These imply that •OH radicals were indeed generated in the system and confirming the degradation of acid blue 25 dye.
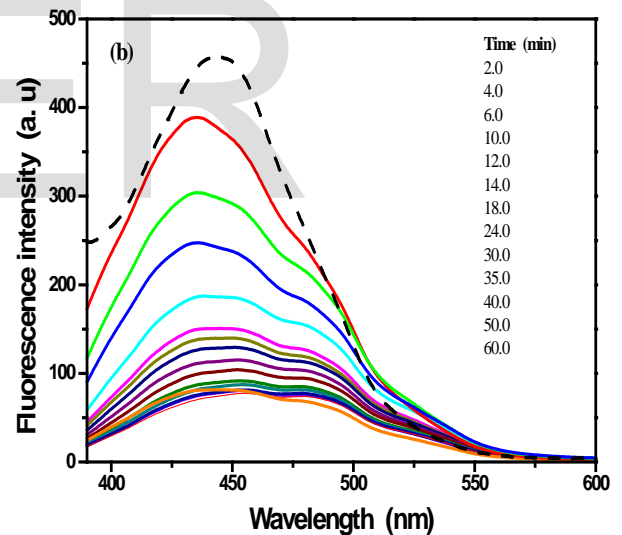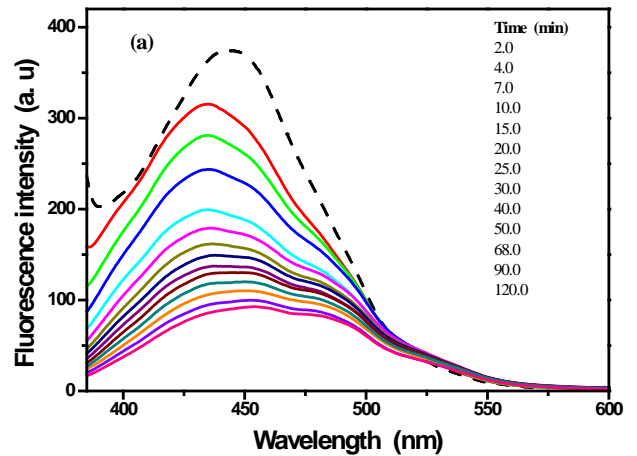

Fig.9. Time resolved emission spectra during reaction of $2×10^{-4}$ M of acid blue 25 dye in the presence of (a) 0·01 g of the complex as heterogenous catalyst (a) and (b) 0·01 g of the complex as a heterogenous catalyst with 0.2 M of H_2O_2.

In order to check the reusability of the Cu(II)-chalcone complex as a catalyst. After the end of degradation process, the complex was collected by filtration, washed with doubled distilled water, and dried at room temperature. The catalyst was reused at the same conditions as discussed above. It was found that the catalyst maintained its catalytic activity for two cycles of the dye oxidation with hydrogen peroxide. After the second cycle, the catalytic activity decreases. The degradation of the acid blue 25 was observed

with UV-visible spectra for 6 hrs and Fig.10, while in comparison with that for the fresh complex, acid blue 25 was completely degraded after 50 min.
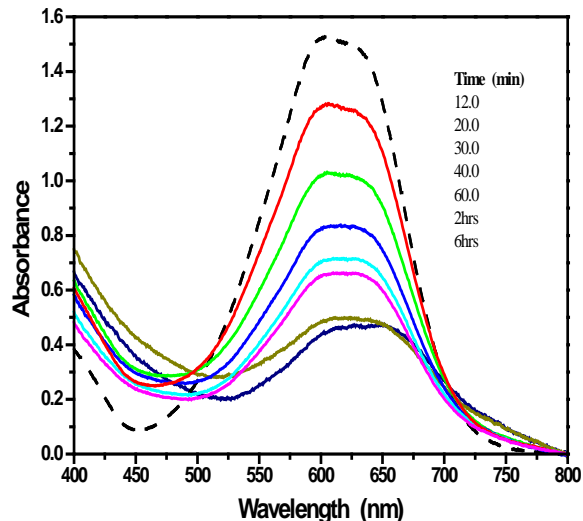

Fig.10. Time resolved absorption spectra for the catalytic activity of the used complex for two cycles of the acid blue 25 dye oxidation with H_2O_2.

4. CONCLUSIONS

1.   Polarization data shows that the investigated inhibitors act as mixed-type inhibitor in 1 M HNO_3.

2.   Double layer capacitances decrease with respect to blank solution when the inhibitor added. This fact may explained by adsorption of the inhibitor molecule on the copper surface.

3.   The values of inhibition efficiencies obtained from the different independent techniques showed the validity of the obtained results

4.   Copper-chalcone complex was used as heterogeneous catalyst for the degradation of acid blue 25 dye.

5.   Addition of H_2O_2 to the system made the degradation of the dye much faster. It was found that the percent of degradation for H_2O_2+catalyst was 86.7. However, the corresponding one with catalyst only was 74.6. Fluorescence technique confirms the degradation process.

6.   The investigated catalyst maintained its catalytic activity for two cycles of the dye oxidation with hydrogen peroxide. The degradation of the acid blue 25 was observed with UV-visible spectra for 6 hrs, confirming the reusability of the investigated complex.

REFERENCES

[1]   H.Y. Ma, C.Yang, B.S.Yin, G.Y.Li, S.H.Chen, J.L.Luo, Electrochemical characterization of copper surface modified by *n*-alkanethiols in chloride-containing solutions, Appl. Surf. Sci. 218 (2003) 144-154.

[2]   E.I. Sayed, M. Sherif, Effects of 2-amino-5-(ethylthio)-1,3,4-thiadiazole on copper corrosion as a corrosion inhibitor in 3% NaCl solutions, Appl. Surf. Sci. 252 (2006) 8615-8623.

[3]   A. Ganesan, K. Kuppusamy, S.V. Shanmuga, G. Mayakrishnan, R. Arumugam, Chemical and electrochemical investigations of high carbon steel corrosion inhibition in 10 % HCl medium by quinoline Chalcones, Ionics. 19 (2013) 919-932.

[4]   A.S. Fouda, A.A. El-Shafie, H.S. Gadow, The use of Chalcones as corrosion inhibitors for nickel corrosion: in nitric acid solution, Port. Electrochim. Acta. 20(2002)13-23.

[5]   C. Kustu, K.C. Emregul, O. Atakol, Schiff bases of increasing complexity as mild steel corrosion inhibitors in 2M HCl, Corros.Sci.49 (2007) 2800-2814.

[6]   A.S. Fouda, M.A. Elmorsi, A. El-mekkawy, Eco-friendly Chalcones derivatives as corrosion inhibitors for carbon steel in hydrochloric acid solution, Afr. J. Pure Appl. Chem. 7 (2013) 337-349.

[7]   M. Behpour, S.M. Ghoreishi, M. Salavati Niasari, B. Ebrahimi, Evaluating two new synthesized S-N Schiff bases on the corrosion of copper in 15% hydrochloric acid , Mater. Chem. Phys.107 (2008) 153-157.

[8]   A.R. Miron, C. Modrogan, O. D.Orbuleṭ, C. Costache, I. Popescu, Treatment of acid blue 25 containing wastewaters by electrocoagulation, U.P.B. Sci. Bull., Series B. 72 (2010) 93-100.

[9]   A.K. Golder, N. Hridaya, A.N. Samanta, S. Ray, Electrocoagulation of methylene blue and eosin yellowish using mild steel electrodes, J. Haz. Mat 127 (2005) 134-140.

[10] A. Archna, K.N Lokesh, R.R. Siva Kiran, Biological methods of dye removal from textile effluents - A review, J Biochem Tech. 3 (2012).

[11] M. Kharub, Use of various technologies, methods and adsorbents for the removal of dye, J. Environ Res Develop, 6 (2012) 879-883.

[12] M. Kulkarni1, P. Thakur, Photocatalytic degradation and mineralization of reactive textile azo dye using semiconductor metal oxide nano particles, Int J Eng Res Gen Sci. 2 (2014) 245-254.

[13] A.S. Stasinakis, Use of selected advanced oxidation processes (AOPS) for wastewater treatment – a mini review, Global NEST J. 10 (2008) 376-385.

[14] P. Verma, P. Baldrian, F. Nerud, Decolorization of structurally different synthetic dyes using cobalt(II)/ascorbic acid/hydrogen peroxide system, Chemosphere. 50 (2003) 975–979.

[15] T. Watanabe, K. Koller, K. Messner, Copper-dependent depolymerization of lignin in the presence of fungal metabolite, pyridine, J.Biotech. 62 (1998) 221–230.

[16] J. Gabriel, V. Shah, K. Nesměrák, P. Baldrian, F. Nerud, Degradation of polycyclic aromatic hydrocarbons by the copper(II)-hydrogen peroxide system, Folia Microbiologica. 45 (2000) 573–575.

[17] I.A. Salem, Kinetics of the oxidative color removal and degradation of bromophenol blue with hydrogen peroxide catalyzed by copper(II)-supported alumina and zirconia, Appl. Cat B. 28 (2000) 153–162.

[18] H. Ghodbane, O. Hamdaoui, Intensification of sonochemical decolorization of anthraquinonic dye Acid Blue 25 using carbon tetrachloride, Ultrasonics Sonochemistry. 16 (2009) 455–461.

[19] D. Chakrabortty, S. Sen Gupta, Photo-catalytic decolourisation of toxic dye with N-doped titania: A case study with Acid Blue 25, J. Environ. Sci. 25 (2013) 1034–1043.

[20] M.N El-Nahass, D.M Abd El-Aziz, T.A Fayed, on-off-on" switchable chemosensor for metal ions detection and its complexes, Sens & Actua: B Chem. 205 (2014) 377–390.

[21] R.G. Parr, D.A. Donnelly, M. Levy, M. Palke, Electronegativity: the density functional viewpoint, J. Chem. Phys 68 (1978)3801-3807.

[22] H. Ma, S. Chen , L.Niu, S. Zhao, Inhibition of copper corrosion by several Schiff bases in aerated halide solutions, J. Appl. Electrochem 32(2002) 65-72.

[23]   J. Aljourani , K. Raeissi, M.A. Golozar, Benzimidazole and its derivatives as corrosion inhibitors for mild steel in 1M HCl solution, Corros. Sci 51 (2009)1836-1843.

[24] H. Amar, A. Tounsi, A. Makayssi, A. Derja, J. Benzakour, A. Outzourhit,

Corrosion inhibition of Armco iron by 2-mercaptobenzimidazole in sodium chloride 3% media, Corros.Sci 49(2007) 2936-2945.

[25] M.A .Migahed, E.M.S Azzam, S.M.I. Morsy, Electrochemical behaviour of carbon steel in acid chloride solution in the presence of dodecyl cysteine hydrochloride self-assembled on gold nanoparticles, J. Corros.Sci 51 (2009) 1636-1644.

[26] M.N.H. Moussa, A.A. El-Far, A.A El-Shafei, The use of water soluble hydrazones as inhibitors for the corrosion of c-steel in acidic medium, J.Mater.Chem.Phys 105(2007) 105-113.

[27] M. Benabdellah, R. Touzan, A. Aouniti, A.S. Dafali, S. El-Kadiri, B. Hommouti, M. Benkaddour, Inhibitive action of some bipyrazolic compounds on the corrosion of steel in 1 M HCl Part I: Electrochemical study, J.Mater.Chem.Phys 105 (2007) 373-379.

[28] E.Bayol ,K. Kayakirilmaz and M. Erbil, The inhibitive effect of hexamethylenetetramine on the acid corrosion of steel, J.Mater.Chem.Phys 104 (2007)74-82.

[29] O.Benalli, L. Larabi, M. Traisnel, L. Gengembra, Y. Harek, Temperature Effect on Corrosion Inhibition of Carbon Steel in Formation Water by Nonionic Inhibitor, J. Appl. Surf. Sci 253 (2007) 6130-6139.

[30] I. Epelboin, M. Keddam, H. Takenouti, Use of impedence measurements for the determination of the instant rate of the metal corrosion, J. Appl. Electrochem 2 (1972) 71-79.

[31] J. Bessone, C. Mayer, K. Tuttner, W. J. lorenz, AC-impedance measurements on aluminum barrier type oxide films, J. Electrochim. Acta 28 (1983)171-172.

[32] R.W .Bosch, J. Hubrecht, W.F. Bogaerts, B.C. Syrett, Electrochemical frequency modulation: A new electrochemical technique for on-line corrosion, J. Corrosion 57(2001) 60-70.

[33] F. Samie, J. Tidblad, , V. Kucera, C. Leygraf, Atmospheric corrosion effects of HNO3 method and results on laboratory exposed copper, Atmospher. Environ 39 (2005) 7362-7373.

[34] F. Samie, J. Tidblad, V. Kucera, C. Leygraf, Atmosphoric corrosion effects of HNO3 – influence of concentration and air velocity on laboratory exposed copper, Atmospher. Environ 40 (2006) 3631-3639.

[35] I. Lukovits, K. Palfi, E. Kalman, LKP Model of the Inhibition Mechanism of Thiourea Compounds, Corrosion, 53 (1997) 915-919.

[36] R. Azmat, Z. Khalid, M. Haroon, K.P. Mehar, Spectral Analysis of Catalytic Oxidation and Degradation of Bromophenol Blue at Low pH With Potassium Dichromate, Advances in Natural Science. 6 (2013) 38-43.

[37] B. Hu, J. Zhou, X-M.Wu, Decoloring Methyl Orange under Sunlight bya Photocatalytic Membrane Reactor Based on ZnO Nanoparticles and Polypropylene Macroporous Membrane, Int J. Poly Sci. (2013) 1-8.

[38] W.X. Zhang, H. Wang, Z.H. Yang, F. Wang, Colloids Surf. A 304 (2007) 60-64.

[39] X. Peng, I. Ichinose, Manganese oxyhydroxide and oxide nanofibers for high efficiency degradation of organic pollutants, Nanotechnology 22 (2011) 015701.

[40] W. Zhang, Z. Yang, X. Wang, Y. Zhang, X. Wen, S. Yang, Catal. Commun. 7 (2006) 408-412.

[41] A. Mehrdad, B. Massoumi, R. Hashemzadeh, Kinetic study of degradation of Rhodamine B in the presence of hydrogen peroxide and some metal oxide, Chem. Eng. J. 168 (2011) 1073-1078.

[42] K.K. Senapati, C. Borgohain, K.C. Sarma, P. Phukan, Photocatalytic degradation of methylene blue in water using CoFe 2O4-Cr2O3-SiO2 fluorescent magnetic nanocomposite, J. Mol. Cat A. 346 (2011) 111–116.

[43] G. Tabbì, S.C. Fry, R.P. Bonomo, ESR study of the non-enzymic scission of xyloglucan by an ascorbate-H2O2-copper system: the involvement of the hydroxyl radical and the degradation of ascorbate, J . Inorg. Biochem . 84 (2001) 179–187.